

Development of Direct Thrust Measurement System for the Completely Electrodeless Helicon Plasma Thruster^{*)}

Daisuke KUWAHARA, Yushi KOYAMA, Shuhei OTSUKA, Takamichi ISHII, Hiroki ISHII, Hiroaki FUJITSUKA, Shimpei WASEDA and Shunjiro SHINOHARA
Tokyo University of Agriculture and Technology, 2-24-16 Naka-Cho, Koganei, Tokyo 184-8588, Japan

(Received 19 November 2013 / Accepted 17 February 2014)

In order to establish a completely electrodeless electric thruster, we have been studying the proposed electromagnetic acceleration methods, and estimating plasma performance using various diagnostics. Plasma thrust is the most important feature of the thruster; therefore estimation of the plasma thrust is necessary. In this study, we have developed a pendulum-target-type plasma thrust stand. Our experiment uses a Large Mirror Device and a high-power radiofrequency source (7 MHz, ~5 kW) to produce high-density helicon plasma. The thruster uses both permanent magnets and electromagnets for generating magnetic field with a large radial component to increase electromagnetic acceleration by the proposed method of including an azimuthal current. In this paper, details of the developed thrust stand and experimental results for thrust, thrust efficiency and specific impulse are presented.

© 2014 The Japan Society of Plasma Science and Nuclear Fusion Research

Keywords: electric thruster, helicon plasma, electrodeless acceleration, thrust measurement, pendulum-target type thrust stand, active damper

DOI: 10.1585/pfr.9.3406025

1. Introduction

An electric thruster is an indispensable propulsion method for long-term missions such as deep-space exploration owing to their high specific impulse. However, electric thrusters, e.g., ion engines, Hall thrusters and magnetoplasmadynamic (MPD) thrusters, have a problem with erosion of generation and acceleration electrodes due to direct contact with plasmas. Therefore, to extend the lifetime of a thruster, it is essential to eliminate direct contact between electrodes and plasmas. To solve this problem, we have been studying a helicon plasma thruster as the Helicon Electrodeless Advanced Thruster (HEAT) project [1]. Our object is to develop a completely electrodeless electric thruster.

The objective of the proposed helicon plasma thruster is outlined as follows. First, generate a dense source plasma using a helicon wave [2] with an excitation frequency between that of ion and electron cyclotrons applied from the outside of a discharge cylinder (non-contact with plasma) using a radio frequency (RF) antenna. Second, in order to achieve a high thrust, accelerate the dense plasma by the Lorentz force F_z using the product of the induced azimuthal current j_θ and the static radial magnetic field B_r . There are several methods proposed in our HEAT project for exciting j_θ in the plasma, and our laboratory is promoting schemes that use two types of coils: rotating magnetic field (RMF) coils [1, 3] and an m (azimuthal mode num-

ber) = 0 coil [1, 4]. Here, B_r is generated using a combination of permanent magnets, which have relatively larger B_r components, and electromagnets surrounding a discharge cylinder. Using either the combined magnetic field configuration or the permanent magnets, we have succeeded in generating high-density ($>3 \times 10^{12} \text{ cm}^{-3}$) Ar plasmas on a Large Mirror Device (LMD, Fig. 1 (a)) [5], and have observed larger increases in the ion flow velocity and the electron density than by using only electromagnets.

To verify our acceleration schemes, plasma diagnostics such as plasma thrust, ion flow velocity, and density measurements in plasma are required. The LMD can accommodate above-mentioned measurements. However, thrust calculations using these measurements produce only indirect values. Therefore, a direct thrust measurement method is required for developing acceleration schemes. We developed a direct thrust measurement system that uses a pendulum-type thrust stand with a cylindrical target [6]. The structure of target-type thrust stand is very simple, and it allows for the attachment of magnets, the discharge cylinder and the RF antenna. It is a good solution for measuring the thrust of a large-diameter, complex and heavy system such as the LMD. Requirements of the thrust stand are as follows, measurement range: 1 - 30 mN, resolution: 0.2 mN, repetition time: ~10 s, high resistance to high-density plasma, and a highly accurate calibration method.

2. Experimental Setup

Figure 1 (a) shows a schematic diagram of the LMD. Considering a divergent magnetic field to be applied in the

author's e-mail: dkuwahar@cc.tuat.ac.jp

^{*)} This article is based on the presentation at the 23rd International Toki Conference (ITC23).

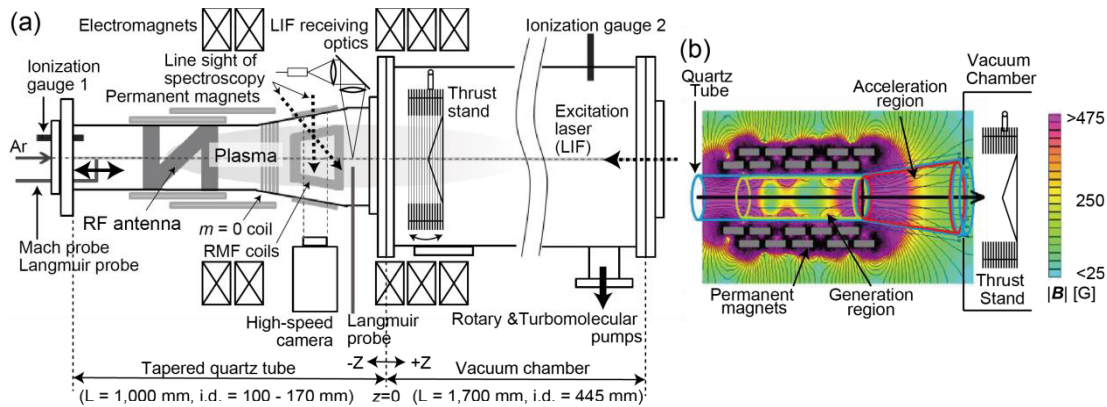


Fig. 1 Schematic of LMD and thrust stand (a) and magnetic field by permanent magnets (b).

acceleration scheme, a quartz tube [1,000 mm in length, 100 - 170 mm in inner diameter (i.d.)] has a tapered shape to prevent wall loss of the plasma. The LMD has two turbo-molecular pumps (1,000 l/s and 2,400 l/s) with a base pressure of less than a few times of 10^{-4} Pa. Argon gas is used as the propellant, and a typical discharge pressure is ~ 0.1 Pa. The helicon plasma is generated using RF power via a half-helical antenna. The RF input power P_{rf} and its excitation frequency f_{rf} are ~ 3 kW and 7 MHz, respectively. The typical pulsed discharge duration time is 75 ms with a duty cycle of 5%. The external magnetic field is applied by 12 sets of electromagnets (not used in this paper). In order to increase B_r , specialty designed permanent magnets were also installed. Figure 1 (b) shows location of permanent magnets and its magnetic field. As to acceleration antennas, RMF and $m = 0$ coils are put on a tapered quartz tube position where the strong B_r is obtained. For plasma measurements, Langmuir probes and Mach probes are used to obtain electron density n_e and argon ion velocity v_i , respectively. Also optically measurement, such as spectroscopic method and LIF one are utilized as non-disturbance measurement. Here, typical values of LMD plasma are as follows. n_e : $10^{18} - 10^{19} \text{ m}^{-3}$, v_i : < 3 km/s, gas flow rate (\dot{r}) of Ar gas: 20 - 70 sccm.

3. Thrust Stand

Figure 2 shows detailed schematic views of the plasma thrust stand. The thrust stand measures the plasma thrust by a displacement of the target structure using a displacement sensor (IL-S025, Keyence CO., reproducibility: $1 \mu\text{m}$). The cylindrical-target is hanged with a low resistance and a low friction by the use of two spikes (target side) and two dimples (upper support side). Since spikes, dimples and the vacuum vessel are well organized each other, the hinge structure can accept target coil current as a completely force-free condition. The target consists of a corn-shape end plate with a 60 degree span from the thruster axis in outer diameter (o.d.) of 320 mm, and a series of 14 thin disks, 240 mm i.d. and 320 mm o.d. with a thickness of 0.3 mm. The distance between neighbor-

ing disks and the end plate is 9.5 mm. Produced ions and neutral particles ejected from the quartz tube enter the target, then collide and reflect by the corn-shape end plate, and reflected particles enter to gaps of disks. Since particles collide with disks many times, they transfer their axial momentum mv (m : particle mass, v : axial velocity) to the target (inelastic condition). Whole structures of target are made of SUS316, with a consideration of a non-magnetization and heat resistance against the high-density plasma. Since the targets are made of SUS316, its weight reaches up to 2 kg.

Most thrust stands have a damping mechanism to reduce mechanical vibration. However, in the case of our thrust stand, there is no damper with sufficient sensitivity against the large mass. Therefore, instead of a passive damper, this stand has an electromagnetic brake that has advantages described below. The electromagnetic brake in Fig. 2 (d) consists of two coils and a differential power amplifier. One coil is installed at the bottom of the target and the other in front of the target coil mounted on the vacuum vessel. The currents feeding both the coils are generated by signals from the displacement sensor through the differential power amplifier. The magnetic force between the two coils stops the target by the negative feedback.

Figure 2 (e) shows time evolutions of waveforms in cases with and without brake-coil currents. When the brake coil is switched off, the amplitude of the displacement does not decrease, because the damping term is small. Therefore, we can calculate the force using the displacement without using a motion equation. When the coil current is switched on, the vibration is suppressed immediately. This enables us to repeat experiments with a short repetition interval.

Furthermore, the two coils can be utilized as a calibration tool with a well-known force. The electromagnetic force between the two coils was measured using an electric balance and precision current sources. A calibration equation relating impulse and displacement was derived from the displacement when pulse currents that produce a known impulse are applied to the two coils. Fig-

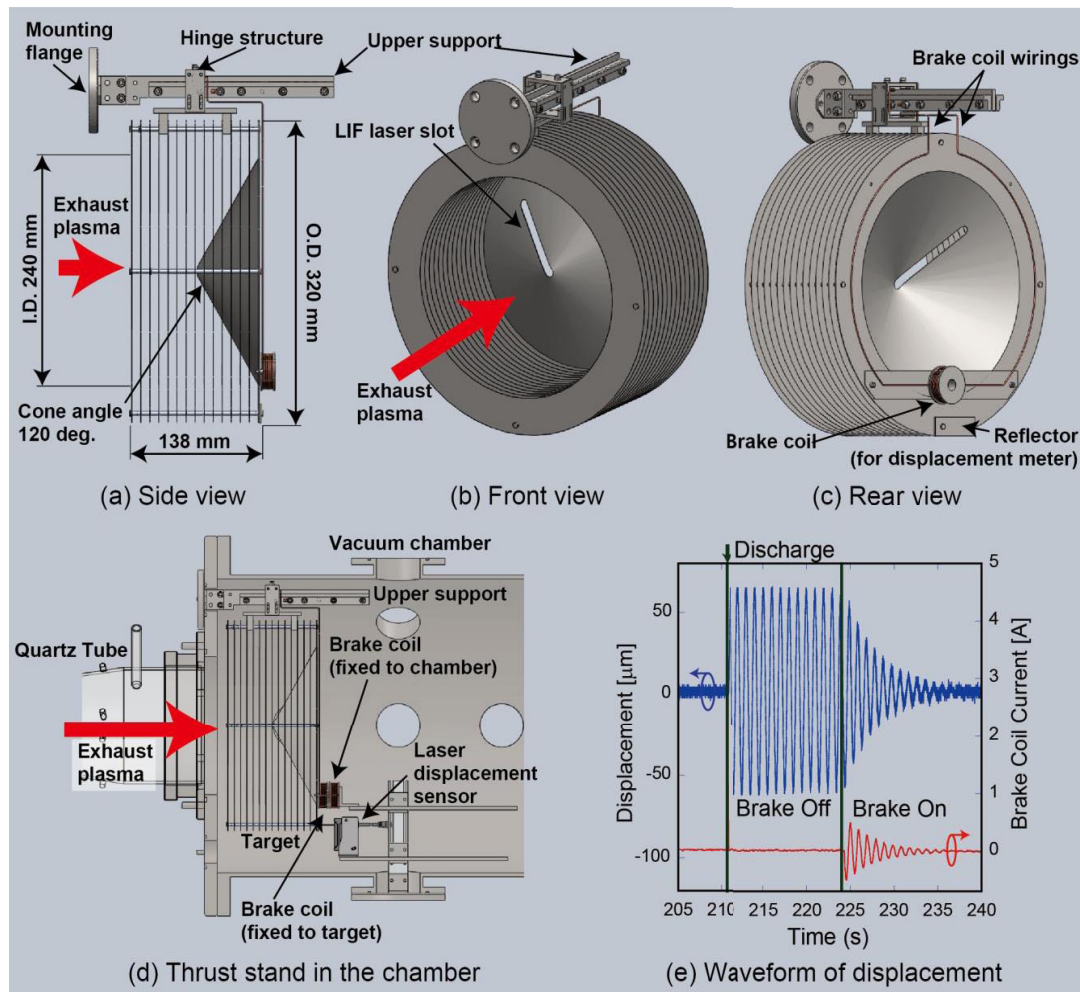


Fig. 2 Details of the thrust stand and waveform of the displacement.

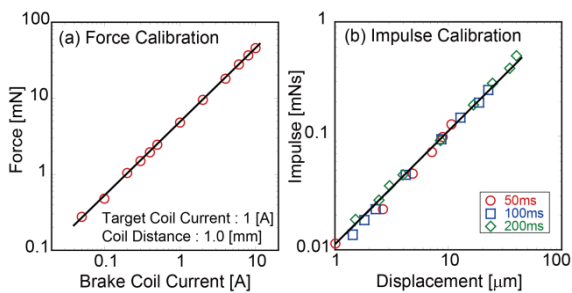


Fig. 3 Calibration results.

Figure 3 shows results of a calibration experiment using two coils. Figure 3 (a) shows the force between the two coils. In Fig. 3 (b), impulses generated by three different duration times (50, 100 and 200 ms) and different currents were applied. According to these calibration experiments, the calibration equation was derived as:

$$F = 1.1 \times 10^{-2} x/T \text{ [mN]}, \tag{1}$$

where F , x , and T are thrust [N], displacement [μm], and duration time of impulse [s], respectively, and the resolution of the thrust was ~ 0.2 mN for a 75-ms discharge.

4. Thrust Measurement

Here, preliminary results of thrust measurement using only permanent magnets are presented. Figure 4 (a) shows that the thrust increased with P_{rf} regardless of the gas flow rate. The maximum thrust obtained is approximately 7 mN with RF power of 2.8 kW and a gas flow rate (\dot{m}) of 50 sccm. Figure 4 (b) shows the thrust efficiency, defined as the thrust divided by the input power. In the case of $\dot{m} = 20 - 50$ sccm, this efficiency is increased by increasing P_{rf} . However, with a high gas flow rate, e.g., 60 - 70 sccm, the efficiency was nearly constant. Figure 4 (c) shows that the specific impulse I_{sp} (thrust per unit mass of propellant consumed per unit time and gravity acceleration) increased monotonically due to an increase in the input power. Here, I_{sp} is calculated by the thrust and gas flow rate ($I_{\text{sp}} = F/\dot{m}g$). The maximum I_{sp} obtained is approximately 1,000 s with RF power of 2.8 kW and \dot{m} of 20 sccm.

5. Discussion

Here, we estimate plasma thrust and specific impulse by the use of the value plasma parameter. The thrust is defined as

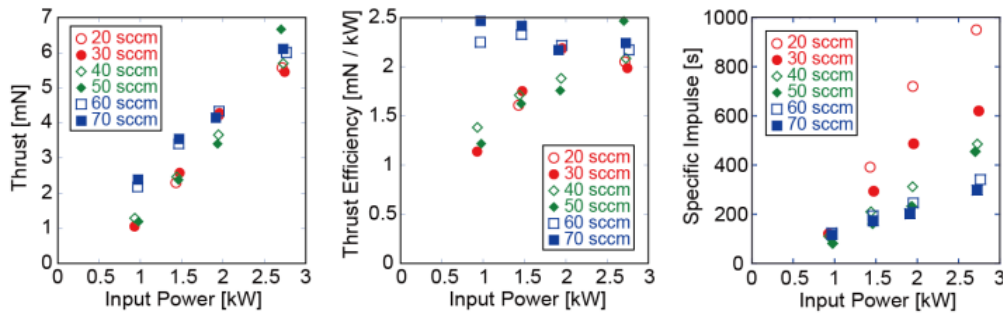


Fig. 4 Results of thrust measurements.

$$F = n_i m_i v_i^2 \pi r^2 \quad [\text{N}], \quad (2)$$

where n_i , m_i , and r denote the ion density, the mass of the ions (Ar), and the plasma radius, respectively. Here, the contribution of neutral particles is neglected. According to Langmuir probe and LIF measurements, typical value of n_i (average ion density) and v_i are taken as $\sim 10^{18} \text{ m}^{-3}$ and 2.4 km/s, respectively. In this case, the RF power and fr were 3,000 W and 25 sccm, respectively. Using those values with $r = 8.5 \text{ cm}$, the thrust is calculated to be 8.7 mN.

These thrust values are nearly the same as those from another helicon plasma thruster [7]. However, for observing I_{sp} , it may be necessary to consider “backward” gas flow, from the open mouth of the quartz cylinder. In addition, the above-mentioned formula did not consider the contribution of neutral particles. In order to determine the net plasma thrust, the thrust stand must be located closer to the generation area.

Observed thrusts, obtained by the thrust stand and calculated from measurements of v_i (LIF) and n_i (Langmuir Probe) are substantially equal, although we have an uncertainty in the momentum thrust, e.g., measuring the 2- mv momentum in the target-type thrust stand [6]. One reason is as follows. The shape of the magnetic field formed by permanent magnets is divergent, i.e., it has a large B_r component. Therefore, most ions collide with the inner wall of the quartz discharge tube, and do not reach the open mouth of the thrust stand. To prove this, it is necessary to form the magnetic field with the additional use of electromagnets, so the field lines do not touch the inner wall of the discharge tube, or the thrust stand must be located nearer to the source plasma.

6. Conclusion

In order to estimate the plasma performance in our

proposed electrodeless propulsion scheme, a thrust stand was developed along with some experimental measurements. The thrust stand has an active brake system using two small electromagnets to maintain high sensitivity and for calibration. The thrust resolution is $\sim 0.2 \text{ mN}$ (for a 75- μs discharge).

As a preliminary result, thrusts were measured under various input RF power and gas flow rates. The largest values are as follows. Thrust: 6.7 mN at fr of 50 sccm and P_{rf} of 2.8 kW, thrust efficiency: 2.5 mN/kW at fr of 70 sccm and P_{rf} of 1.0 kW, and specific impulse: 950 s at fr of 20 sccm and P_{rf} of 2.8 kW. It was confirmed that thrust values observed by the thrust stand are nearly the same as calculated one.

Acknowledgement

The authors would like to thank the late Prof. K. Toki and the late Prof. K. P. Shamrai for their great contributions to our HEAT project. We also appreciate the useful discussions between HEAT project members. This research has been supported by Grants-in-Aid for Scientific Research (S: 21226019) from the Japan Society for the Promotion of Science.

- [1] S. Shinohara, H. Nishida, T. Tanikawa, I. Funaki and K.P. Shamrai, *Trans. Fusion Sci. Technol.* **63**, 16 (2013).
- [2] R.W. Boswell, *Phys. Lett.* **33A**, 457 (1970).
- [3] I.R. Jones, *Phys. Plasmas* **6**, 1950 (1999).
- [4] S. Shinohara, T. Hada, T. Motomura, T. Tanaka, T. Tanikawa, K. Toki *et al.*, *Phys. Plasmas* **16**, 057104 (2009).
- [5] S. Shinohara, S. Takechi and Y. Kawai, *Jpn. J. Appl. Phys.* **35**, 4503 (1996).
- [6] M. Coletti, A. Balestra, M. Sensimi and G. Paccani, *Proc. 30th Int. Electric Propul. Conf., IEPC-2007-158* (2007).
- [7] K. Takahashi, C. Charles and R.W. Boswell, *Phys. Rev. Lett.* **110**, 195003 (2013).